Multi-scale slope instabilities along the Nile deep-sea fan, Egyptian margin: A general overview

Lies Loncke [a,*], Virginie Gaullier [a], Laurence Droz [b], Emmanuelle Ducassou [c], Sébastien Migeon [d], Jean Mascle [d]

[a] Laboratoire IMAGES—E.A. 3678, Université de Perpignan, Bâtiment U, 2ème Etage, Via Domitia 52, Avenue Paul Alduy, 66860 Perpignan, France
[b] UMR 6538, Institut Universitaire Européen de la Mer, Place Nicolas Copernic, 29280 Plouzané, France
[c] Université Bordeaux 1, UMR-CNRS 5805—EPOC "Environnements et Paléoenvironnements Océaniques", Avenue des facultés, 33405 Talence Cedex, France
[d] Géosciences Azur, UMR 6526, OOV, B.P.48 - 06235 Villefranche-sur-Mer, Cedex, France

ARTICLE INFO

ABSTRACT

The Nile deep-sea fan (NDSF), turbiditic system reaching a size of about 90,000 km^2, has been investigated since 1998 by several geophysical methods (multibeam bathymetry, backscatter imagery, seismic data, 3–5 kHz echo-sounding). The analysis of this important data set evidenced that the NDSF is the locus of numerous multi-scale slope instabilities. Three main types of instabilities have been defined, mainly on the basis of their size or origin. (1) First type of instabilities related to the generalized gravity spreading of the Plio-Quaternary deep-sea fan on Messinian salt layers. This global spreading is accommodated by numerous localized slides. (2) Second type of instabilities correspond to giant mass movements probably triggered either by earthquakes, fluids, or climate and eustatic oscillations. Finally, (3) third type of instabilities correspond either to localized levee liquefactions or to thin-skinned slides on the steep slopes of the Eratosthenes seamount. The deposits generated by these slope movements greatly participate in the building of the NDSF. The characterization of these different instabilities, in a petroleum province as the NDSF, has important implications in terms of risk assessments when considering drilling operations.

© 2008 Elsevier Ltd. All rights reserved.

1. Introduction

Continental margins are the locus of two main types of gravity-transport processes: gravity flows (including turbidity currents and debris flows) and submarine landslides, both being sometimes related. Massive slope instabilities are increasingly recognized to contribute for an important part of deep-sea fans building and in maintaining the overall gradient of the continental slope. Moreover, slope instabilities remobilize large volumes of sediments, which can cause great human and material damage (cable breaks, tsunamis). When planning industrial drilling operations, the analysis of landslides also becomes an important issue. The study of distribution and triggering parameters of slope instabilities has thus strong social and economic implications. It is in particular crucial to understand how submarine landslides look like, where and in what kind of geological setting they occur, in order to infer the triggering factors and the time of their occurrence.

The Nile deep-sea fan (NDSF) on the Egyptian passive margin has been intensively surveyed since 1998 by Géosciences Azur using mainly multibeam bathymetry and backscatter imagery, 3.5 kHz echo-profiling and seismic reflection data. This data set has been a very powerful aid in understanding the construction and evolution through time of that deep sedimentary system (Gaullier et al., 2000; Mascle et al., 2000; Bellaiche et al., 2001; Loncke, 2002; Loncke et al., 2002; Loncke and Mascle, 2004; Loncke et al., 2006). Data analysis enhanced in particular the importance of salt-related tectonics on the regional structure of the fan, the existence of numerous seepage structures (gas chimneys, pock-marks, mud volcanoes) and a great variability of sedimentary processes.

This paper, focusing on the various types of slope instabilities participating in the NDSF shaping and evolution, first gives an overview of the distribution, extension and relative frequency, of recent (Late Pleistocene–Holocene) slope instabilities on the basis of bathymetric and 3.5 kHz and seismic data analysis. Some of these events are calibrated by cores (Ducassou et al., 2006; Ducassou et al., 2007). Giant debris flows discovered on high-resolution and industrial seismic data, are then analysed, in terms of geometries, relative timings and influence on the sedimentary evolution of the Rosetta part of the NDSF (Western fan). These results allow finally discussion of possible triggering parameters and potential damage risks along the Nile margin.

* Corresponding author. Tel.: +33 4 68 66 17 45; fax: +33 4 68 66 20 19.
  E-mail address: lies.loncke@univ-perp.fr (L. Loncke).

2. Previous work

2.1. Geological framework

The NDSF is a 2/3 km thick sedimentary wedge constructed chiefly since Late Miocene by terrigenous sediment delivered by the Nile River (Salem, 1976; Dolson et al., 2000). The NDSF covers a segment of an old passive margin believed to have initiated from successive rifting episodes in Jurassic and Early Cretaceous times (Biju-Duval et al., 1978; Morelli, 1978; Hirsch et al., 1995).

Today the sub-aerial Nile delta shows two main fluvial/sedimentary pathways: the western Rosetta branch and the eastern Damietta branch (Fig. 1). The fluvial deltaic system extends offshore from the Rosetta branch across a wide continental shelf (80 km average width). With the exception of the major indentation related to the Rosetta canyon, the Egyptian continental shelf is a flat and undeformed domain, only characterized, particularly in its eastern corner, by gentle, probably sandy, hydraulic dunes, caused by a general east-directed long shore drift (Bellaiche et al., 2001). A major deep-sea fan, covering the continental slope and abyssal plain (down to 3500 m water depth), formed at the foot of this wide platform; it shows a very variable morphology controlled by combined interactions between salt tectonics and various mechanisms of sediment distribution, including turbidite dispersal, giant slumps and debris flows (Gaullier et al., 2000; Loncke, 2002; Loncke et al., 2006). The sedimentary loading of Messinian ductile salt layers has, in particular, triggered spectacular salt-related tectonic deformations (Ryan and Hsü, 1973; Gaullier et al., 2000; Loncke, 2002; Loncke et al., 2006), similar to those commonly seen on salt-bearing passive margins (Worall et al., 1989; Diegel et al., 1995; Trudgill et al., 1999; Rowan et al., 1999; Vendeville, 1999; Cramez and Jackson, 2000; Stover et al., 2001; Vendeville and Jackson, 1992a,b). Gravity spreading and gliding of the salt and overlying sediments has induced proximal thin-skinned extension along the shelf and the upper slope and distal contraction along and at the base of the continental slope. In parallel, numerous mud volcanoes revealing active fluid seeping shape the NDSF (Loncke and Mascle, 2004).

2.2. Morphostructural characteristics of the NDSF

From west to east, and on the basis of its overall morphology, the NDSF has been divided onto three distinct provinces (Fig. 1).

(1) *The western province*. The western province of the NDSF is probably the best-documented part of the Egyptian margin, from the platform area down to the abyssal plain. Many analyses enhanced that this part of the NDSF is the most active in terms of turbidite deposition, at least since 130,000 years (Maldonado and Stanley, 1979; Bellaiche et al., 2001; Loncke, 2002; Ducassou et al., 2006; Ducassou et al., 2007). In that area, a canyon deeply incised the continental slope (the Rosetta canyon, Fig. 1), allowing important sediment bypasses to the abyssal plain where extensive sandy lobes have been recognized on backscatter imagery. The Rosetta Fan, connected to the Rosetta canyon shows a series of recently abandoned and active well-ramified channel–levee systems, through which turbidites sediments have been and are still transported nearly 300 km from the shelf edge. The continental slope of this province is crossed by a curved belt of growth faults that localize the upslope extent of the Messinian mobile deposits. Toward the north, the channel–levee systems and distal lobes are progressively incorporated onto the Mediterranean Ridge accretionary prism (Loncke et al., 2002; Huguen, 2001).

(2) *The central province* does not display any prominent canyon nor continuous deep-sea channels, but is rather characterized by a chaotic seafloor surface interpreted as a result of repeated sedimentary instabilities (Loncke et al., 2002; Newton et al., 2004). These instabilities seem to have covered or dislocated older channel–levee systems (Pleistocene in age after Abdel Aal et al., 2000). In this area most of the evaporite-rooted growth faults appear to have been sealed except at the east where a 150 km long E–W trending belt of still active growth faults runs along the upper continental slope. At the base of the slope, this province is bounded by a series of contractional folds resulting from salt tectonics.

(3) *The eastern province* shows a strong contrast with the previous ones and correlates with a NW–SE directed tectonic corridor that is more than 200 km long and almost 100 km wide.
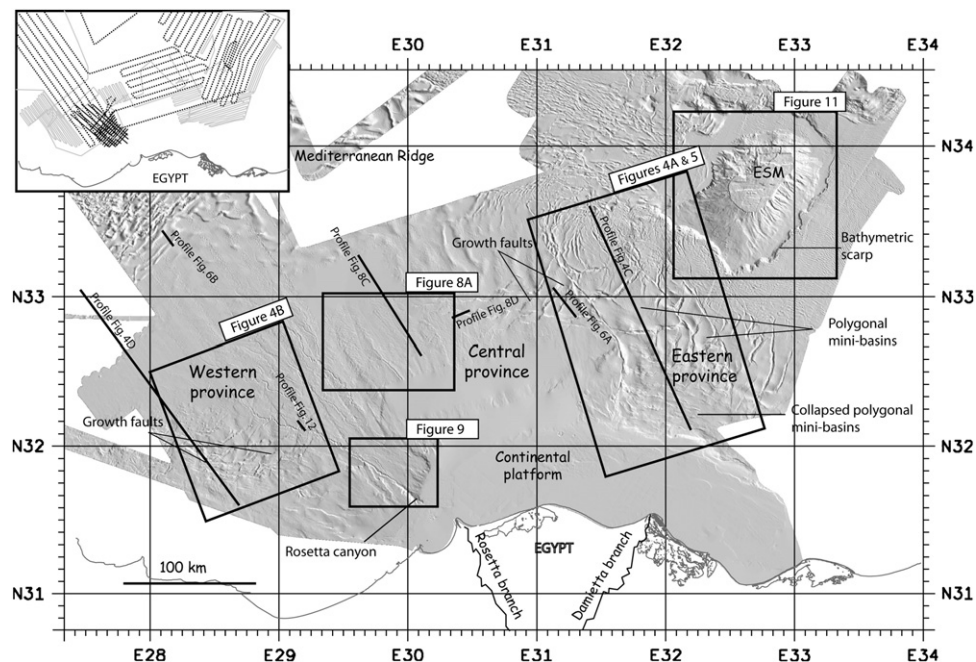

Fig. 1. Shaded bathymetry of the Nile deep-sea fan (NDSF), from a compilation of EM12, EM300 multibeam bathymetric data and 3D seismic first arrivals (BP-Amocco). ESM, Eratosthenes Seamount. On the left corner are the corresponding tracklines. Dotted black lines: Prismed II survey (6 channel streamer seismic data + bathymetry + 3–5 kHz profiler). Grey lines: Fanil survey (24 channel streamer Seismic data + bathymetry). Black lines: seismic data from BP-Amocco.

This corridor is bounded on both sides by linear and narrow fault zones (Gaullier et al., 2000; Mascle et al., 2000; Loncke et al., 2006). Within this belt, numerous small collapsed polygonal basins are seen upslope. These mini-basins are anchored on pre-Messinian sequences as a consequence of massive salt withdrawal; they are inactive. Midslope, crestal grabens, bounding non-collapsed depocentres, are detected, while Messinian evaporites are progressively stacking and thickening downslope where they create curved salt ridges and a wedge of short-wavelength folds (Loncke, 2002; Loncke et al., 2006). The eastern NDSF is bounded by an important seamount of continental origin: the Eratosthenes seamount (ESM) (Robertson, 1998). Its very specific flat-topped shape is directly related to the Messinian salinity crisis that strongly eroded the seamount. Its gullied slopes probably also relate for a part to this event. Its surface is deformed by a set of E–W normal faults (Sage and Letouzey, 1990) probably resulting from the bending and uplift of ESM undergoing subduction processes near Cyprus arc. The freshness of these faults suggests very recent tectonic activity. This seamount has been very poorly sedimented since Messinian times (maximum thickness of 0.5 s twtt (seconds two way travel time) on top of the seamount), probably because of its height, preventing turbiditic sedimentation. The contact between the deep-sea fan itself and the seamount is marked by an important bathymetric scarp corresponding to the distal tip of Messinian evaporites, just as for the Sigsbee escarpment, in the Gulf of Mexico (Gaullier et al., 2000; Loncke et al., 2006). In the eastern part of the NDSF, the structural evolution has been significantly influenced by the proximity of the Eratosthenes Seamount. This large topographic buttress has served to both limit and deflect the northeastwards allochthonous advance of the Messinian evaporites, and this has severely complicated the deformational pattern of the overlying Plio-Quaternary sedimentary cover (Loncke et al., 2006). East of Eratosthenes seamount, the seafloor surface is gently folded, again resulting from progressive gliding/spreading of sediments on Messinian evaporites. There, salt-bearing sequences are rather thin, only covered by a few hundred meters of Pliocene to Quaternary sediments, and dissected by few channels, probably partly originating from the Levantine coast (Bellaiche et al., 2001).

2.3. Recent sedimentation (Late Pleistocene–Holocene)

Various studies based on piston-coring or echo-sounding techniques allowed clarification of the recent sedimentary characteristics of the NDSF (Ross and Uchupi, 1977; Maldonado and Stanley, 1979; Cita et al., 1984; Reeder et al., 1998; Rebesco et al., 2000; Loncke et al., 2002; Ducassou et al., 2006). Echo-character studies documented the predominance of turbiditic bedded echo-types and disturbed echo-types generated by mass-wasting processes. Regional piston core studies revealed a general transition from fine-bedded prodeltaic deposits on the upper slope to turbidite-rich sequences on the deep-sea fan. Core studies also showed that the marine domain of the Nile consists principally of clays and silts, with secondary sandy, carbonated, and sapropelic deposits.

In the Western province, sedimentation rates are high, especially in the offshore extension of the Rosetta branch (average rates of 32 cm/1000 yr after Maldonado and Stanley (1979) for the last 58,000 years and even 280 cm/1000 yr in distal parts (lobes) of the fan, during terminal Pleistocene after Ducassou et al., 2006), where the highest proportion of turbidite accumulations occurs and the sandy deposits are concentrated. The activity of gravity flows resulted in a well-developed network of meandering deep-sea channels. The size and depth of the channel–levee systems decreases downslope in the lower fan regions. In contrast to the acoustically well-stratified middle fan regions, the deposits in the lower fan regions return very rough sea floor echo-types and are

characterized by high reflectivities on backscatter maps, indicating the presence of widespread coarse deposits of sandy nature.

The central province is mainly characterized by hemipelagic sediments (Maldonado and Stanley, 1979). Some fossil channels exist downslope (at ~2500 m water depth) but have been dislocated upslope. Average sedimentation rates are in this province of the order of 2–4 cm/1000 yr for Late Pleistocene, Holocene times.

In the eastern province, cored sediments exhibit a high variability of facies, including debris flows and turbidites. Muddy turbidites constitute however a low proportion of the sediments and are interbedded in pelagic and hemipelagic sediments (Ducassou et al., 2006), confirming that the Damietta part of the NDSF is mostly inactive since 127,000 years, as already suggested by the scarcity and dissected nature of the channels in that part of the fan. Average sedimentation rates are of 6 cm/1000 yr (Late Pleistocene/Holocene).

3. Data set

Three successive academic geophysical/geological surveys (Prismed II, Fanil and Vanil) have been carried out on the NDSF by Géosciences-Azur laboratory since 1998 providing continuous bathymetric and backscatter images of the NDSF, by using Simrad EM12-Dual and EM300-Dual multibeam sounding systems (Fig. 1). During these surveys, deep sub-bottom structures, at penetration sometimes up to 3 s twtt, were also imaged using a 75-inch^3 Sodera GI gun and a six-channel streamer. High resolution seismic data (24-channel streamer) was acquired to image channel–levee systems especially in the western NDSF. Very high-resolution 3.5 kHz profiles were also collected on a major part of the study area. A total of about 5000 km of continuous geophysical data has been obtained over most of the NDSF (see track lines on Fig. 1). Several gravity and piston cores have also been collected on the survey area but will not be presented in this paper (see Ducassou, 2006; Ducassou et al., 2006; Ducassou et al., 2007). Our data set has been completed, in some specific key areas, by (1) upper sections of a few multi-channel seismic data and coherency maps provided by BP-Egypt (Fig. 1), and (2) 3.5 kHz data collected during Nautinil cruise (2002), part of Mediflux European program.

It is important to note that although some pleistocene mass-wasting events are still expressed on the present-day seafloor, some others cannot be fully imaged on 3.5 kHz data because of low penetration (50–80 m below seafloor, depending on sediment lithology and physical properties) and important sedimentation rates (especially in the Western NDSF). To map buried debris-flows, slumps or slides, we used available seismic data. Because different seismic acquisition systems provide seismic data with different quality, we built a "quality chart" of available seismic data (Fig. 2). Most of the NDSF has been surveyed with seismic data of poor resolution (quality 4). However, for the western part of the NDSF (Fig. 2), high-resolution seismic data are available (mostly qualities 1 or 2) and allowed a constrained analysis. For the upper part of the western NDSF we analysed a set of 31 profiles that were systematically crossed. To strengthen our analysis we favoured interpretations coming from high-resolution profiles.

4. Methods used to recognize slope failures and related deposits

4.1. 3.5 kHz echo-character mapping and analysis of bathymetry

Recent mass-wasting events are generally easy to recognize on bathymetry by the presence of head and footwall scars (McAdoo et al., 2000). In contrast, associated remobilized deposits are more difficult to identify and map especially when events are disintegrative and do not generate clear distal toes. Alternatively, when conserved, debris flows or slump deposits are generally units of
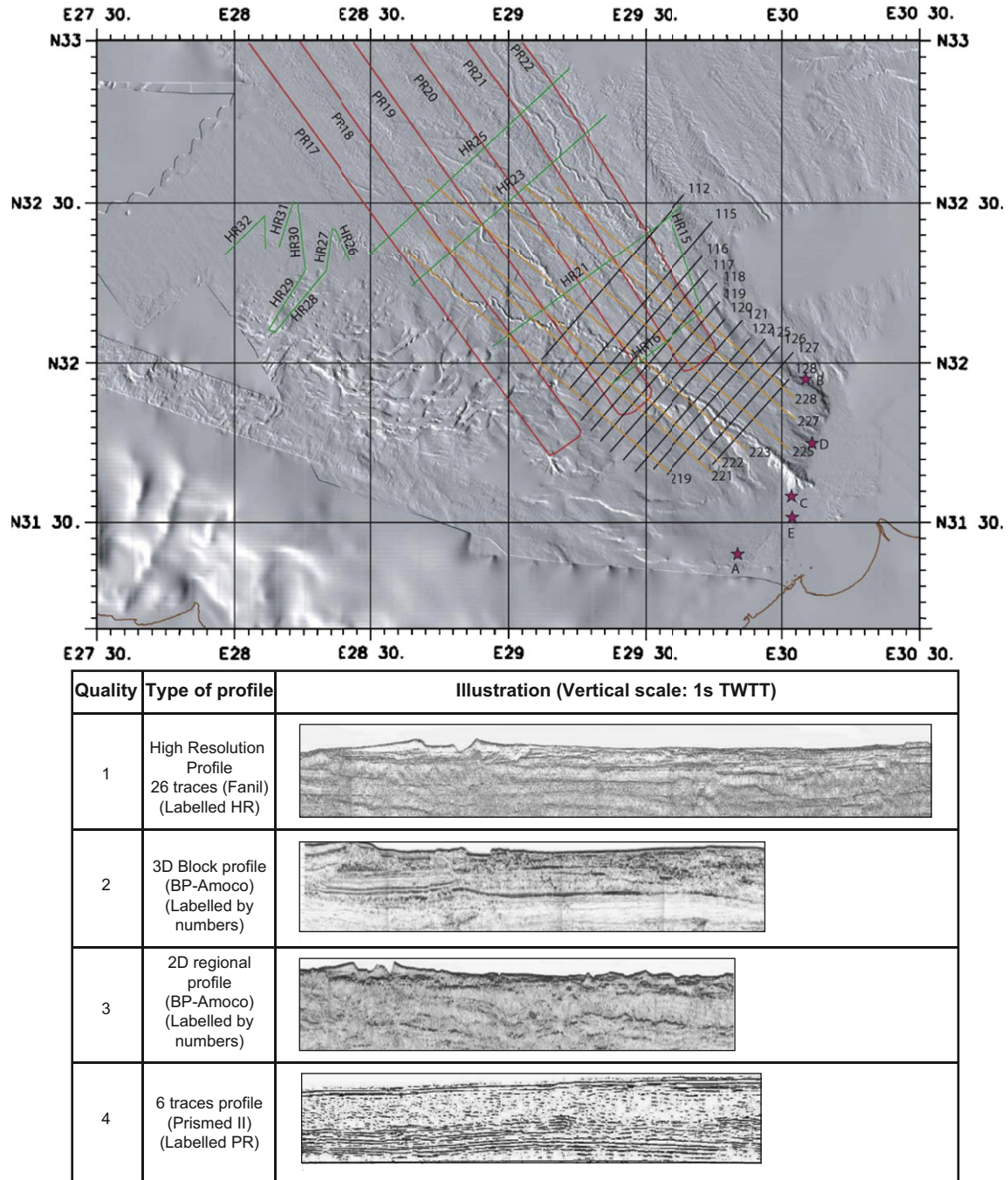
Quality	Type of profile	Illustration (Vertical scale: 1s TWTT)
1	High Resolution Profile 26 traces (Fanil) (Labelled HR)	
2	3D Block profile (BP-Amoco) (Labelled by numbers)	
3	2D regional profile (BP-Amoco) (Labelled by numbers)	
4	6 traces profile (Prismed II) (Labelled PR)	

Fig. 2. Trackline map of seismic data available in the Western province and associated quality chart.

incoherent to transparent character, and analysis of 3.5 kHz data appears very powerful to constrain their extents. Many studies based on comparisons between 3.5 kHz data and piston cores (Damuth and Hayes, 1977; Damuth, 1980b, 1994; Damuth and Flood, 1984; Pratson and Laine, 1989) allowed to settle relationships between echo-character, sedimentary types and depositional processes. Such study has already been carried out for the NDSF and the relative parts of turbiditic and mass-wasting processes have been discussed (Loncke et al., 2002). The following echo-characters are usually considered distinctive of mass-wasting deposits (Fig. 3):

– Hyperbolic echo-characters. These have different meanings depending on the size, shape, and spacing of the hyperbolas. The occurrence of hyperbolas is mainly linked to the roughness

of the seafloor topography and masks the real underlying echo-facies. Large irregular hyperbolas are associated with rough topographies such as seamounts, basement highs, fault scarps and rugged slopes. Small regular hyperbolas (H2, Fig. 3) are commonly associated with gently folded deposits generated by mass-wasting processes (Damuth, 1980a and b, 1994).
– Transparent echo-characters (T1). Most debris-flows return relatively diffuse, fuzzy, almost prolonged echo-types from their upper surfaces. They generally lack coherent internal reflectors, appear acoustically transparent and have erosive bases (Embley, 1976, 1980; Jacobi, 1976; Damuth, 1980a,b, 1994). Anyway, transparent echo-types can correspond also to muddy turbidites (Cita et al., 1984; Tripsanas et al., 2004). In most cases, a geometric analysis of these transparent bodies

allow to distinguish both sediment types: when observed transparent bodies are irregular or lens-shaped and have an erosive base, they most likely correspond to debris-flow deposits. In turn, when transparent bodies tend to drape equally underlying sediments and reliefs and have a conformal contact, they most likely correspond to muddy turbidites. In some cases however, in particular within salt related mini-basins (Tripsanas et al., 2004) or tectonically induced basins as in the Mediterranean Ridge (Cita et al., 1984), some ambiguity exist: transparent lens-shaped bodies can correspond to local catchments of fine-grained turbidites. In such cases, the differentiation in between muddy turbidites and debris flow deposits is impossible without coring.

– Transparent perturbed echo-characters (Tp). Some debris flow deposits are transparent and have disorganized surface echoes, nearly hyperbolic. These surface echoes can be related to blocks diffracting acoustic energy or to surface ripples due to important shear stresses during the movement of the observed sedimentary mass.

– Transparent buried echo-characters (Tb). These correspond to transparent masses buried by bedded turbiditic and/or hemipelagic deposits.

– Chaotic echo-character (C). Chaotic facies commonly correspond to highly disorganized sediments such as debris-flow deposits or slumped sediments (Pratson and Laine, 1989; Damuth, 1994).

– Hummocky echo-character (H) commonly correspond to creeping sediments or sediment-waves. The analysis of the internal geometry of these echoes generally allows one to distinguish both sediment types.

Of course, the correlation between echo-type and sediment type or process is not always so clear. Same sedimentary processes can be expressed by different types of echo-characters on 3.5 kHz data and a specific echo-type can refer to several sediment types. Consequently, the identified echo-types need to be placed in their physiographic and geological context, and if possible to be calibrated by cores, before attempting any correlation to a given sedimentary process. We used bathymetry (shaded or not), backscatter imagery or slope gradient maps to constrain our interpretations.

4.2. Seismic data analysis (for buried events)

On seismic data, the criteria used to recognize remobilized deposits are the following.

The main debrites and remobilized masses are characterized by acoustic transparency (associated with internal destructurations, micro-faulting and presence of fluids) and erosive bases. Their surface appears sometimes undulated (due to important stresses during the remobilization itself). Downslope of these masses, compressional structures are sometimes observed.

Regarding slumps and slides, these are rarely preserved (destroyed by recent events) or imaged by our data-set (most seismic profiles do not reach the preserved footwall scars). In some rare cases, tilted or rotated packages can be observed on seismic data.

5. Results: distribution of slope instabilities on the Egyptian margin

We identified numerous recent slope instabilities in the three provinces of the NDSF on bathymetry or 3.5 kHz and seismic data. Three main types of instabilities have been discriminated and mapped according to their sizes or their controlling parameters.

5.1. Instabilities related to the generalized gravity gliding/spreading of the Plio-Quaternary sedimentary cover on the Messinian salt layers

5.1.1. Structural framework

The western and central provinces are characterized essentially by gravity gliding processes that led to the creation of proximal growth fault belts and distal folds merging with the accretionary Mediterranean Ridge (Fig. 4B and D). The eastern province is mostly characterized by gravity spreading processes that led to a wide variety of salt-related structures, especially upslope where they range from growth faults to crestal grabens bounding mini-basins (Fig. 4) (Loncke et al., 2006). These deformations locally create steep escarpments, especially within in the extensional and contractional domains (Fig. 4). In intra-slope basins and along growth faults, flank oversteepenings are common, due to subsidence of the basins and concomitant uplift of surrounding salt diapirs. In turn, in distal compressional areas, fold uplifts are common due to either purely salt-related compressional forces or deep-seated compressional pulses related to the vicinity of the Mediterranean Ridge. The presence of numerous dissected channels on the sides of crestal grabens, or cached within intraslope basins as well as the "freshness" of scarps and folds suggest recent activity of these gravity-driven features.

5.1.2. The impact of salt-related structuration on the generation of instabilities

We identified numerous instabilities in the vicinity of salt-related structures (Figs. 5 and 6). Since there is sometimes an ambiguity in determining if transparent deposits are muddy turbidites or remobilized deposits in some pounded basins, we determined: (1) established remobilized masses and (2) potential remobilized masses (generally, transparent masses with no erosive base).

5.1.2.1. Established slope instabilities (in red in Fig. 7).
These are essentially recognized on bathymetry. Several slope failures have been mapped, especially in the eastern province, which is considered to be the most active in terms of salt tectonics (Fig. 5). Some of these features appear quite "cohesive" since scarps and distal toes are recognizable (Fig. 5A,C). Others are only identifiable by their scarps, probably because they generated disintegrative debris flows that were trapped within ponded mini-basins (Fig. 5D). Recent piston-core analysis (Ducassou, 2006; Ducassou et al., 2006; Ducassou et al., 2007) confirms that debris-flow deposits are frequently observed in the vicinity of salt-related structures and especially along crestal grabens structures.

Echo-character mapping based on the analysis of 3.5 kHz profiles and seismic data (Loncke et al., 2002 and Fig. 7) evidenced also the presence of numerous acoustically transparent or chaotic deposits in both extensional and contractional domains on the whole deep-sea fan (Fig. 6). The transparent or chaotic deposits, appearing in extensional and compressional domains generally do not exceed 10 m in thickness and have reduced sizes (10 km² on average). The chaotic/transparent echo-types are often located at the foot of growth faults, inside mini-basins, or trapped within basins emplaced between main distal contractional folds (Fig. 7).

5.1.2.2. Possible slope instabilities (in light red in Fig. 7).
Going towards the Mediterranean Ridge (MR) and in the distal part of the eastern NDSF, there is an uncertainty in interpreting transparent echo-types as remobilized deposits. These can correspond either to debris flows or to unifites, i.e. structureless mud deposits related to fine-grained turbidites generated by depositional segregation of large turbidity currents. Cita et al. (1984) identified for example within the Mediterranean Ridge, bedded sediments covered by
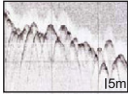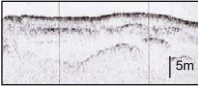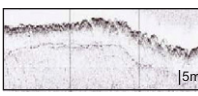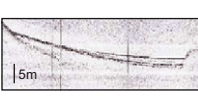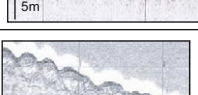
Echo Type	Designation	Interpretation (sediment type)	Sedimentary process
5m	Small regular hyperbolae, H2	Debris flows, creeping masses and levee destabilizations	MASS WASTING (mass flows)
5m	Transparent, T1	Debris flows	MASS WASTING (mass flows)
5m	Transparent perturbed Tp	Debris flows	MASS WASTING (mass flows)
5m	Transparent-Bedded Tb	Succession of glided and turbiditic deposits	MASS WASTING (mass flows) + TURBIDITY CURRENTS (fluidal flows) or HEMIPELAGITES
5m	Chaotic, C	Slumps, debris-flows	MASS WASTING (slides & mass flows)
30m	Hummocky, H	Creeping masses or sediment waves	CREEPING or TURBIDITY CURRENTS

Fig. 3. Classification of 3–5 kHz echo-types commonly related to mass-wasting processes. Vertical exaggeration of the sections is about 30.

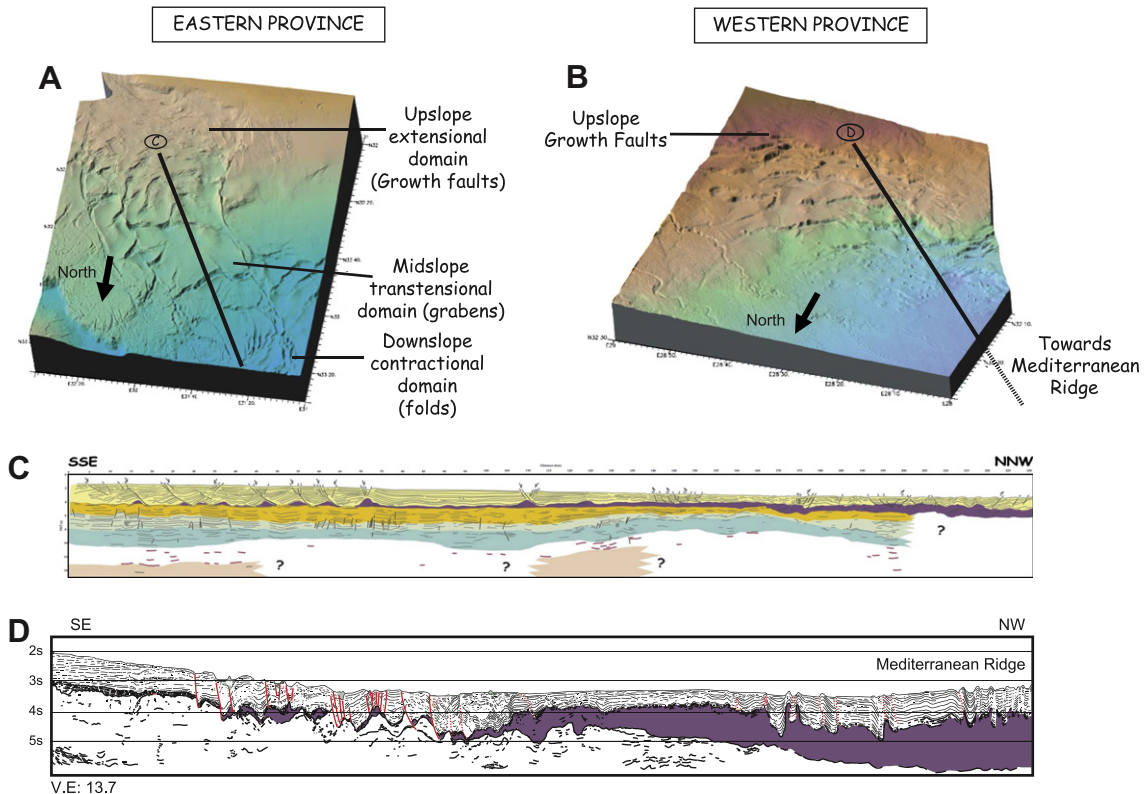EASTERN PROVINCE

WESTERN PROVINCE

Fig. 4. 3D bathymetric blocks and deep penetrating seismic profiles (Médisis survey, interpretation by L. Caméra) showing the style and surface expression of salt-related structures in the Eastern and Western provinces of the NDSF (see location on Fig. 1).
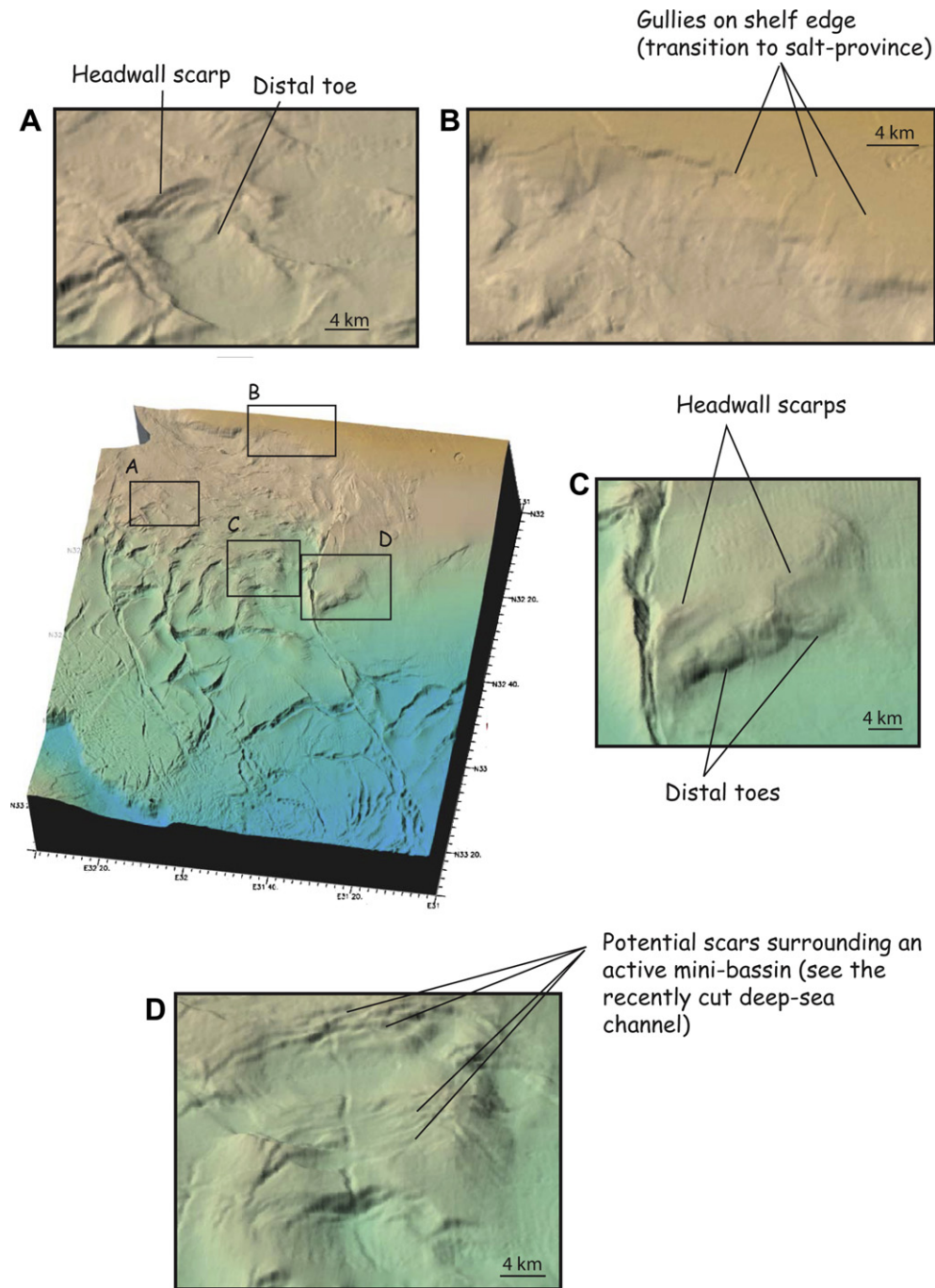
Fig. 5. Bathymetric details on recent slope failures in the eastern province.

transparent layers that have been cored and correspond to muddy turbidites. In our study area, we lack cores to confirm or infirm this hypothesis.

To summarize, the distribution of slope instabilities along salt-related active structures, at least in Late Pleistocene, suggests that remobilized sediments participate significantly to the sedimentation in salt bearing provinces. These events are clearly related to local oversteepenings due to salt-tectonic activity. The compartmentalization of the NDSF salt basin, especially in the eastern province leads to destabilizations and mass-wasting deposits of small extent that seem to be repetitive. In the Gulf of Mexico, sedimentary edifice very similar to the NDSF, Tripsanas et al. (2004) and McAdoo et al. (2000) also recognized bathymetric failures and acoustically transparent units occupying flat basin plains, related to

the collapse of diapirs flanks during episodes of strong salt-tectonic activity. From that first analysis on the NDSF area, it appears that two levels of gravity instabilities are related to the presence of salt: (1) regional gravity spreading or gliding of the salt/sediment system implying the whole Plio-Quaternary system (Fig. 4) and (2) local readjustments implying a few meters, related to these general downslope motions that generate important oversteepenings (Figs. 5–7).

5.2. Giant slope instabilities in the central and Western province

5.2.1. The central province: the central slide complex

In the upslope part of the central province of the NDSF (devoid of mobile salt layers) initiates an important slide complex (more

ARTICLE IN PRESS

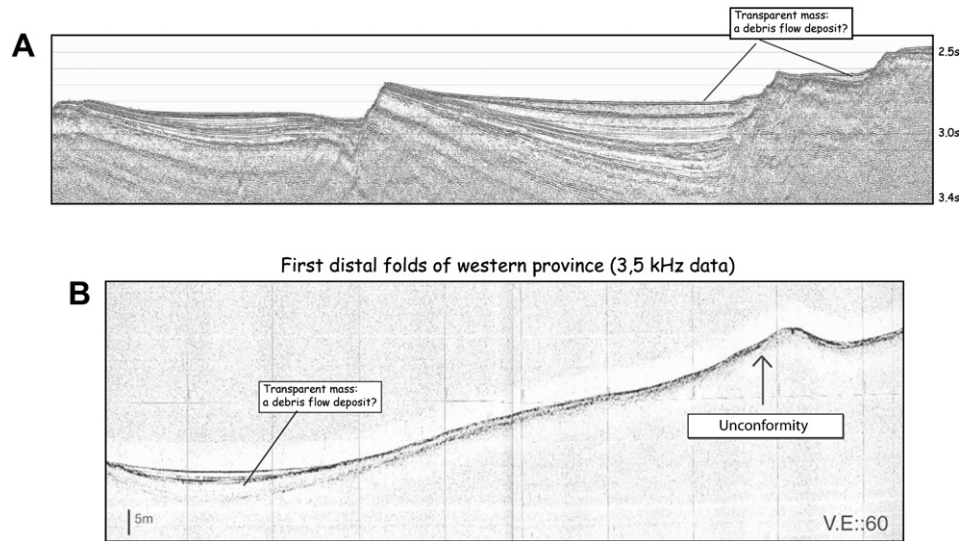8   *L. Loncke et al. / Marine and Petroleum Geology xxx (2008) 1–14*

Fig. 6. Example of acoustic transparent masses. (A) On seismic data in the eastern province; (B) on 3,5 kHz data in the western province (see location on Fig. 1).

than 10,000 km^2 in extent) characterized at its surface by important pock-mark fields (Fig. 7). Only few seismic lines are available in this province, but the observed slide complex seems to be made of several masses and reach depths of 0,2 s twtt.

On 3.5 kHz data, the upslope part of this destabilized belt is characterized by transparent, transparent-perturbed, and chaotic echo-facies (Loncke et al., 2002). The downslope part of this complex is the best imaged by our data-set. On bathymetry, this slope area shows rough, chaotic small-scale reliefs, as well as linear furrows, perhaps disconnecting individual sedimentary flows (Fig. 8). At least a part of these furrows probably corresponds to ancient channels partly covered by mass-wasting deposits. This could explain the fact that nearly no channels are observed in the

upslope part of the Central province, despite the fact that this area has been an important area of turbiditic deposition during Pleistocene times (Abdel Aal et al., 2000). In this downslope part of the slide complex, hummocky echo-characters are prevailing (Figs. 2 and 8). There, the internal sedimentary structure of the surface remobilized unit (25 m in thickness) appears coherent but asymmetrically folded, and the folded unit covers a large buried and transparent debris flows that has been cored and appears highly consolidated. The reflector separating the bedded and folded unit from the transparent unit likely corresponds to a decollement layer. This style of deformations suggests slow spreading of the recent overburden on the top of debris flow (creeping process). Considering that creeping is mainly described as occurring along
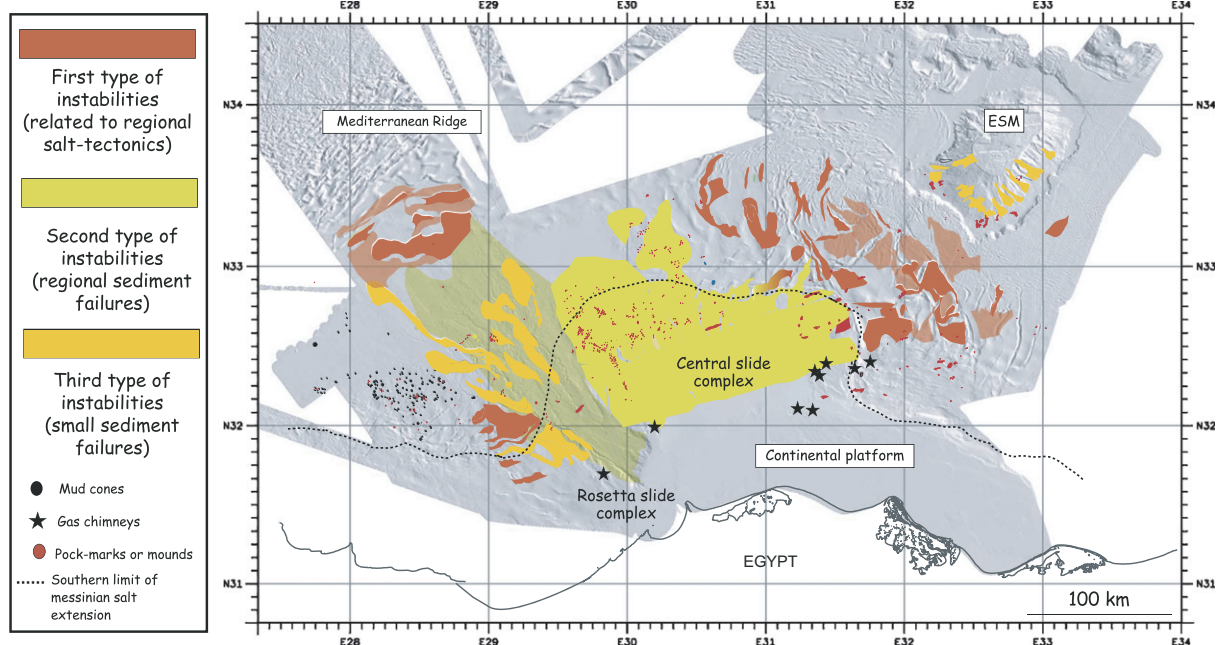

Fig. 7. Distribution map of recent slope instabilities observed on 3–5 kHz data (modified after Loncke et al., 2002). The dotted line corresponds to the southern limit of Messinian salt extension. Different types of fluid ascents are represented on the same map (after Loncke and Mascle, 2004). Notice that for the first order instabilities, established slope deposits are indicated in dark red and possible instabilities in light red.
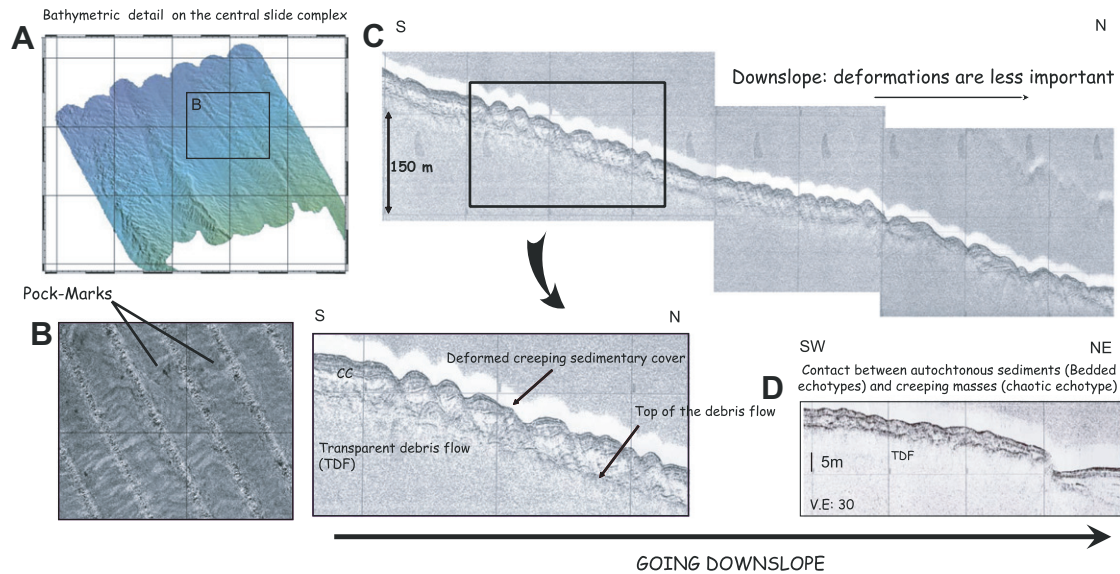
Fig. 8. (A, B) Bathymetry and backscatter imagery focusing on the destabilized area of the Central province. A set of representative 3–5 kHz profiles documents the internal structure of surface sediments probably slowly creeping above an older debris flow (see location on Fig. 1).

geotechnically weak horizons, it is possible that the top of the debris flow has been characterized by important fluid pressures (by dewatering and/or deeper gas ascents), reducing sediment shear strengths. The presence of an important active pockmark field on top of these structures (Fig. 7) (Loncke and Mascle, 2004) attests to important fluid circulations in this area. Also, the close association between destabilized deposits and pockmarks tends to support a relationship between the two phenomena. Considering the potential presence of gas hydrates, for a 13 °C bottom water temperature, as is the case in the study area, hydrates should, theoretically, be stable below around 1900 m of water depth (Sloan, 1990). It is thus possible that, as proposed for many other areas (Bouriak et al., 2000), the emplacement of thick mass-wasting deposits, suddenly overloading the seafloor and modifying pressure and temperature conditions, have induced hydrate dissociation, generating free gas migrations towards the seabed (Pecher et al., 1998; Rempel and Buffett, 1998; Von Huene and Pecher, 1999; Bouriak et al., 2000). "Climatic" generated gas hydrate dissociation could also be responsible for the observed slides and cold seeps as proposed by Praeg et al. (2007) that reprocessed seismic data on site and discovered the presence of a BSR over a depth range of 2000–2500 m, deepening from 220–330 ms below the seabed.

Finally, a recent survey (Nautinil, part of Mediflux program), allowed procurement of additional bathymetry upslope from these deposits, near the initiation area. Many pockmarks and gas chimneys have been described near the headwall of the slides, at about 600 m depth along the shelf break, again suggesting a close relationship between fluids and slope instabilities.

5.2.2. Giant slumps and associated debris-flows in the Western province: The Rosetta slide complex

Even if mass-wasting processes probably significantly participated in the recent past to the edification of the NDSF, resolution limits related to available data do not allow one to recognize well buried mass-wasting deposits on seismic profiles except in the western part of the NDSF where giant slope destabilizations seem to have been very active at least during the last 130,000 years (age estimated from core dating from Ducassou et al., 2007). At the head of the Rosetta canyon, extremely well marked scars, up to 500 m high, and transparent acoustic deposits that are systematically bottomed by an erosional unconformity, reveal the existence of

huge instability processes in that area (Figs. 7 and 9). Moreover, the complexity of associated scar traces suggests multiple events. In order to depict if these transparent packages are related to the failures observed near the Rosetta canyon, an extensive analysis of seismic profiles has been carried out, based on a grid of 31 profiles of various resolutions and qualities (see Fig. 3).

The main result of this analysis is that the Rosetta fan appears constituted for about 30–40% of its thickness, of transparent deposits generated by large slope failures (Figs. 9 and 10). In more detail, the base of the recent Rosetta fan (i.e. about the last 1000 m of sub-bottom sediments) is made of a series of very thick transparent deposits that were generated by slides and/or slumps triggered on the edge of the continental platform as attested by the scars observed on bathymetry and seismic data near the head of the Rosetta canyon (Fig. 9).

In detail, ten episodes of sliding and/or slumping and associated remobilized sediments (Gl-1 to Gl-10 from the oldest to the youngest) were deposited during three main periods intercalated with two periods of turbidite systems deposition (units I and II) (Fig. 10).

(A) The first instability period (Fig. 10A) led to the emplacement of four transparent masses initiated at the shelf break. This period is probably partly responsible for the 30 km long composite scar observed upslope. The sum of these four basal slides and related mass-wasting deposits totals a volume of about 1900 km³. Remnants of the first slide (Gl-1) have been discovered at a latitude of 31°55N (Figs. 9 and 10). The second slide (Gl-2) that probably has remobilized part of Gl-1, is better preserved and related deposits appear more extended northwestwards. On seismic profiles, related transparent mass-wasting deposits seal salt-related growth faults (Figs. 9 and 10). For these two slides (Gl-1 and Gl-2), the initiation area is not known because of remobilisation by the following events Gl-3 and Gl-4. These last two events are probably generated in response to retrogressive erosional processes of the initial failure area. Parts of the initiation area of Gl-3 and Gl-4 have been conserved, and show evidence of slumping processes (rotational faults) (Fig. 9c). At the end of these four events (Gl-1 to Gl-4), we believe that the residual headwall scarps were very close to what is observed nowadays, i.e. a complex and steep headwall, curved in plan view and displaying long side-walls. The fact that the headwall is very steep probably results from the consolidated nature of sediments that were remobilized. Such important slope oversteepening foretells further retrogressive evolution.
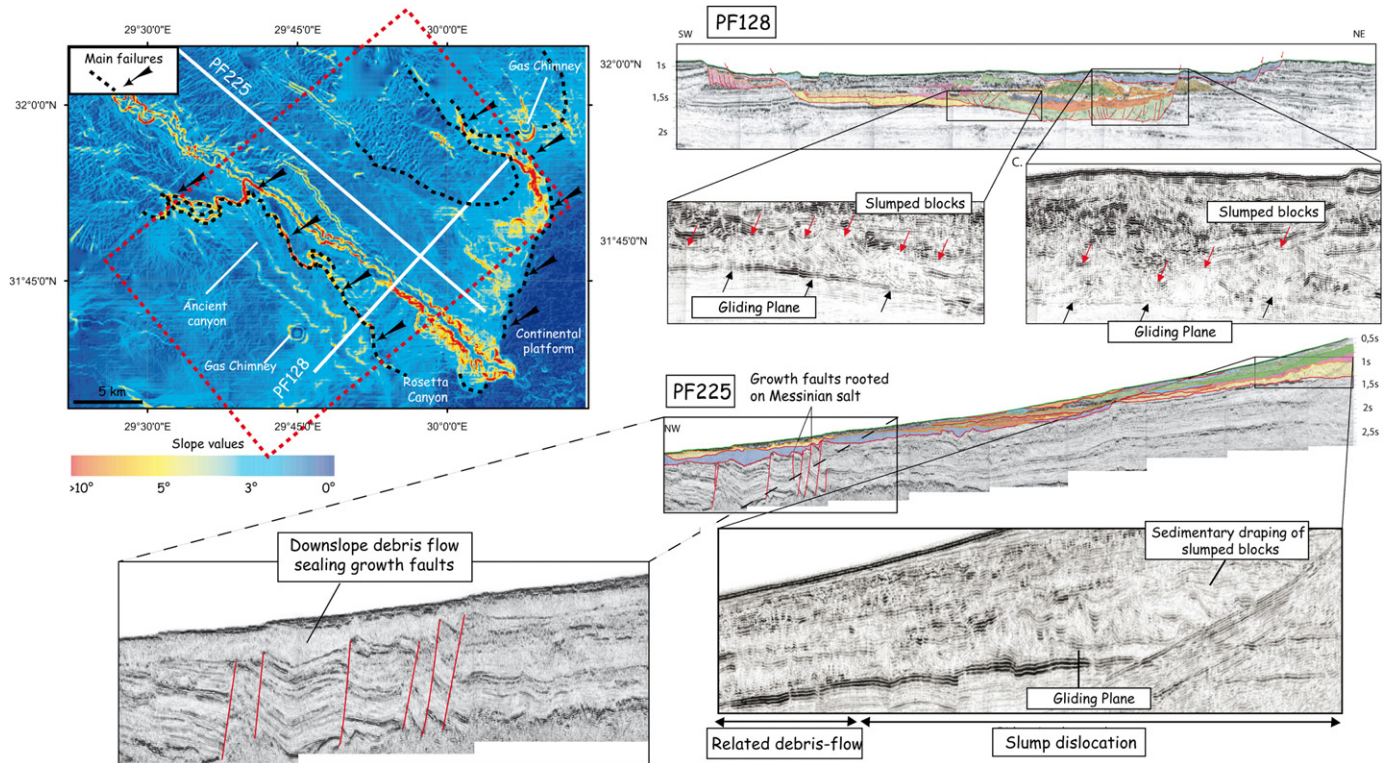
Fig. 9. Slope gradient map of the Rosetta canyon area evidencing different slope failures. Two representative seismic profiles show the structure of the initiation area of slide Gl-4 and related downslope deposits sealing salt-related growth faults (see location on Fig. 1).

(B) These first mass-wasting events resulted in an asymmetrical residual topography, deeper eastwards than westwards that controlled the location of the following turbidite depocentres of seismic Unit I. At least six imbricated channel–levee systems (Ia to If, in order of decreasing age), some of which are still visible on the seafloor, constitute Unit I and occupy the deeper eastern depression (Fig. 10B).

(C) The end of Unit I is marked by erosional transparent layers interpreted as new gliding events (Gl-5 and GL-6) (Fig. 10C).

(D) At this stage of the Rosetta fan history, turbidite deposition to the east had resulted in a residual depression to the west, where a second unit (Unit II) of 10 imbricated channel–levees systems (IIa to IIj in order of decreasing age), including the last active channel, was emplaced (Fig. 10D). As suggested by Bellaiche et al. (2002) from data downfan, a general westwards migration of the channel–levee systems can be evidenced. This westwards migration probably results from the tendency to infill free space. Inside Unit II, transparent deposits (Gl-7 and Gl-8) affect the western parts of channel–levee systems IIe and IIh respectively, and small-scale destabilized deposits can also be observed, either corresponding to salt-related slides or to levee breakings and related avulsion processes.

(E) Finally, two recent mass-wasting deposits (Gl-9 eastwards and Gl-10 westwards) cover part of Unit II (Gl-10 eventually being synchronous of Gl9). Slide Gl-9, observable on bathymetry and marked by a rough topography, clearly attests of the retrogression of the eastern main scar. This slide, which originated in the vicinity of an important gas chimney (Loncke and Mascle, 2004), could have been triggered in part by high pore pressures associated with high gas contents.

Several cores have been collected in some of the landslide units previously described. Some biostratigraphic analyses revealed that the timing of sliding events ranges from about 117 kyr to the Holocene time (Garziglia et al., 2005; Ducassou et al., 2007).

5.3. Small-scale slope failures along the Eratosthenes seamount and active channels

5.3.1. Eratosthenes seamount

The steepness of extremely gullied sides of the Eratosthenes seamount makes the 3.5 kHz data unusable for echo-type analysis. However, bathymetric data and slope gradient maps are very efficient in imaging numerous failures probably resulting from important tectonic activity (Fig. 11). Headwall scars as well as distal compressional toes are generally well expressed, suggesting quite compacted and cohesive material. The slides and gullies seem to erode ESM along successive rims. At the very base of ESM, in particular, northeastwards and southwards, gullies are very fresh suggesting recent erosional processes linked to active uplift (Fig. 11). Finally, while the southern and eastern face of ESM appear affected by numerous thin-skinned gullies, slides and/or slumps, the northwestern flank of ESM seems to have been affected by deeper concave, amphitheatre-like failures caught between two normal faults.

5.3.2. Western active channel (Western province)

Small-scale failures are also identified by the presence of hyperbolic or transparent echo-types on levees of some middle-fan channels in the western part of the NDSF (Fig. 12). In that case, the destabilization of the levees might be induced by sediment failure on channel sidewalls by excessive sediment loading during flow travel path. Furthermore, we noticed that destabilizations are most often recognized on the northern levees, i.e. the levees located downslope, whereas the southern (upslope) levees remain undisturbed. This observation could be explained by the contrasted effect on levees of overflows of turbidity currents: southwards, overflows are directed against the slope gradient and therefore result in a local decrease of the regional slope, forming a stable plateau-like topography. To the contrary, northwards overflows are directed along the slope gradient and result in an oversteepening of the seafloor and, therefore, are more prone to destabilize.
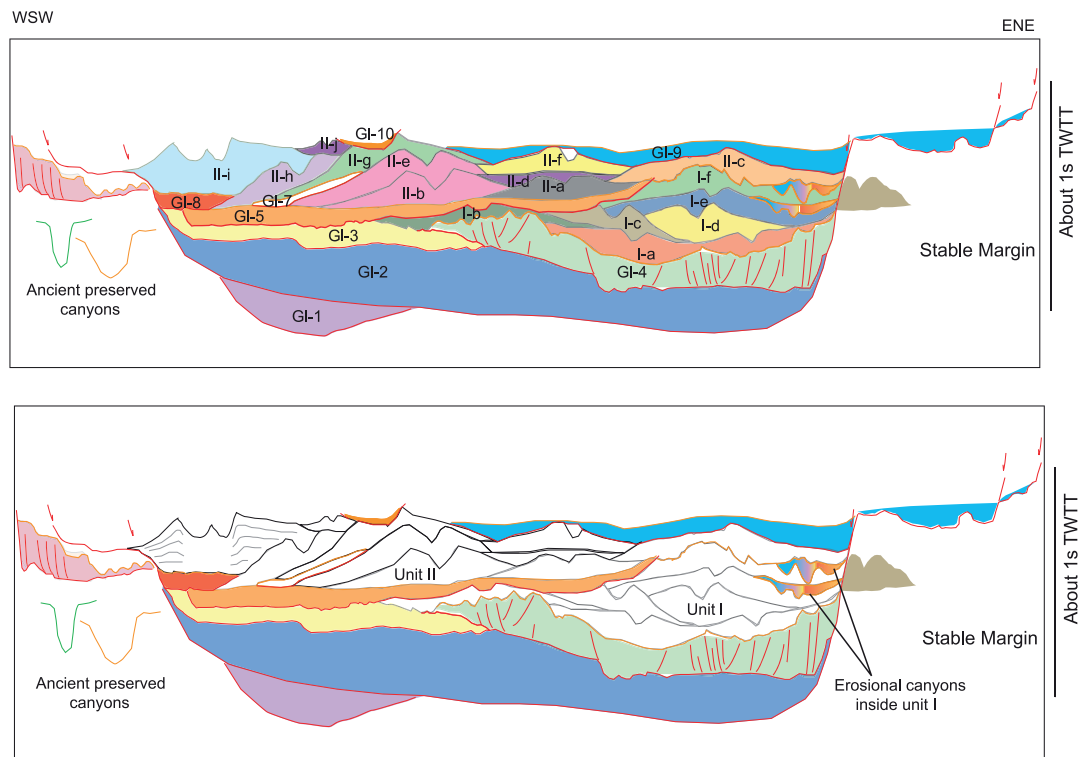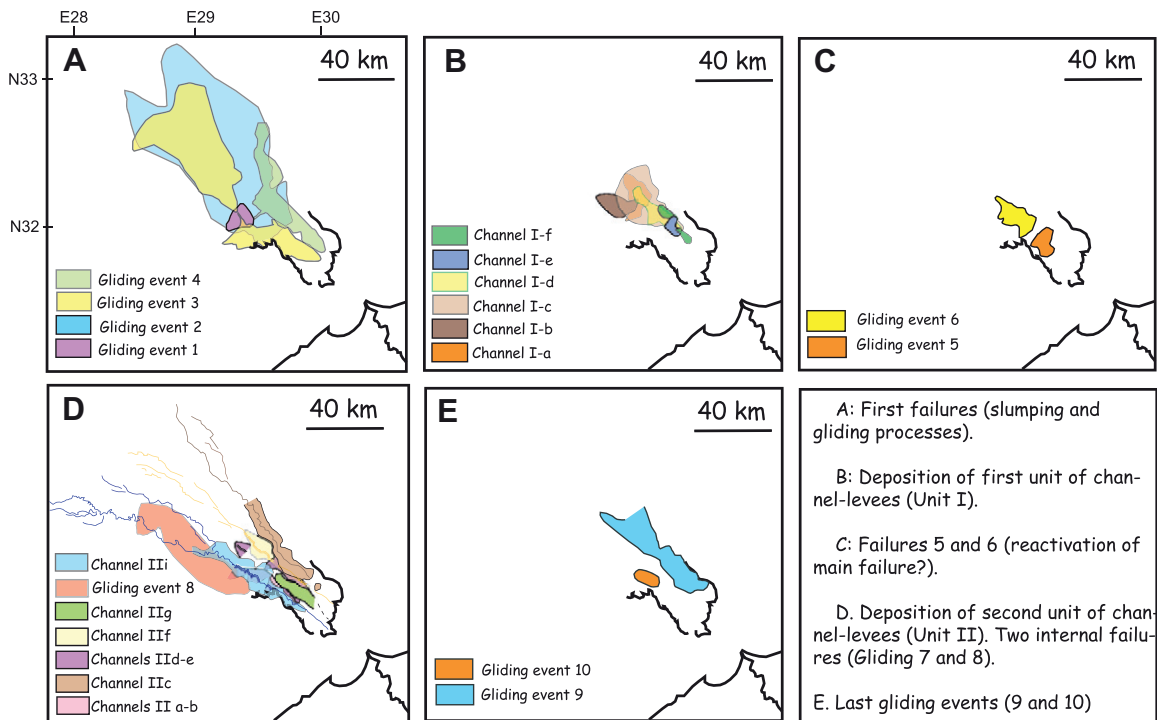
Fig. 10. (A–E) Details represent the main stages of edification of the Rosetta fan. On each sketch, the extension of glided deposits and channel–levee systems are represented. A synthetic cross-section summarizes the geometrical and relative relationships between defined channel–levee units and mass-wasting deposits.

6. Discussion and elements of hazards

Concerning the regional instabilities (central and Rosetta slide complexes), comparisons are difficult both in terms of age and of structure. As a matter of fact, in contrary to the Rosetta slide, the central slide is poorly imaged by seismic data (all available data of "low quality" and miss-oriented) and poorly constrained by core data. Are these slides contemporaneous? Related to differential sedimentary inputs associated with sea-level variations? These questions are still asked.

Anyway, some first conclusions can be settled:

– the central slide complex appears clearly related to fluid ascents even if the genetic relationship between instabilities and fluid ascents is not well constrained. Are the fluid ascents a consequence of important instabilities (themselves related to
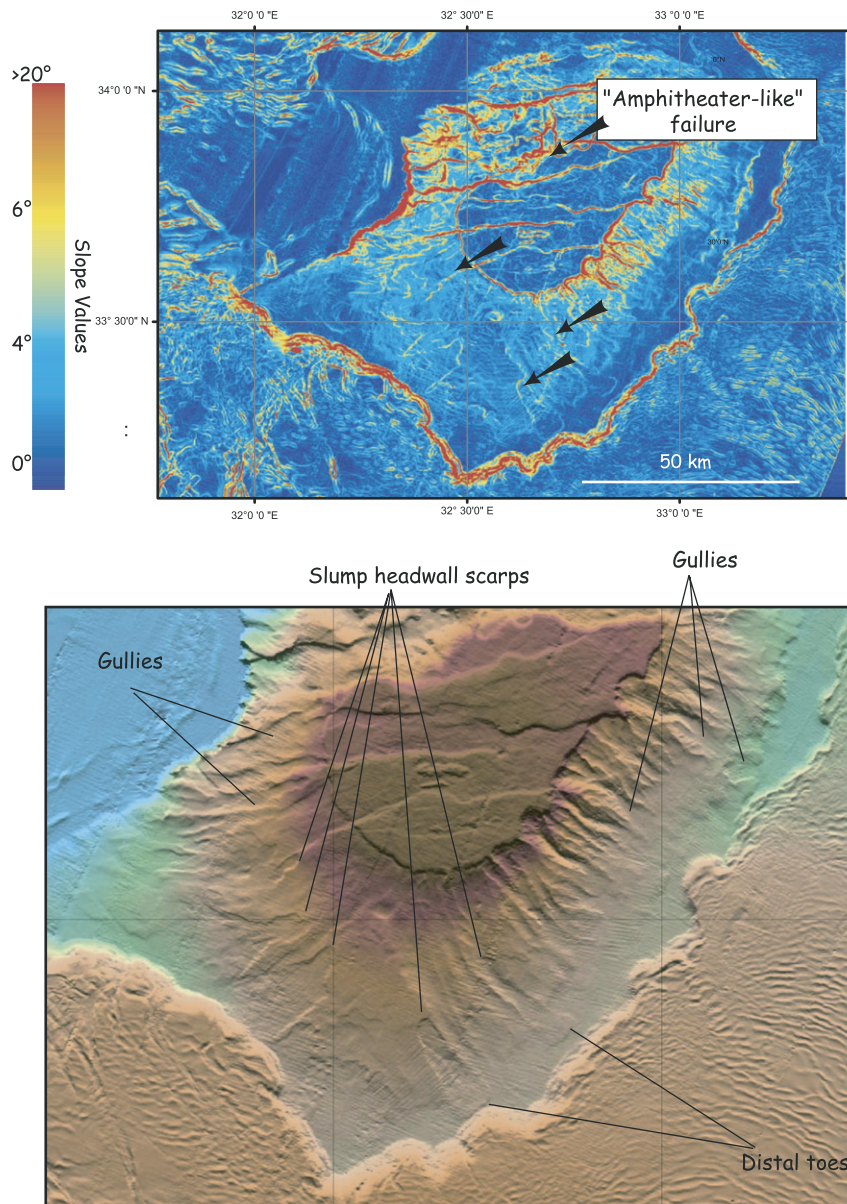
Fig. 11. Slope gradient and bathymetric maps focusing on slope failures observed in the vicinity of ESM (see location on Fig. 1).

variations in sediment input associated with eustatism and climate oscillations, tectonics, or others) or do the fluids result from these large instabilities? The effect of gas hydrates dissociation during glacial-interglacial changes could play a role in this setting (Praeg et al., 2007).

– in the case of the Rosetta slide complex, the main parameters controlling failure are easier to depict, at least in a qualitative
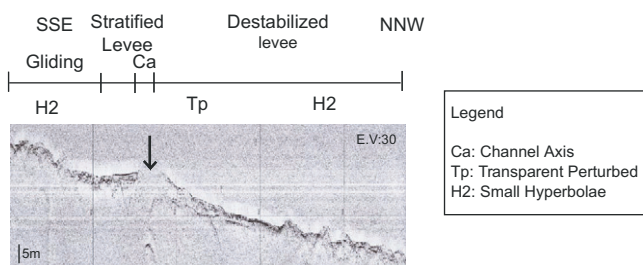

Fig. 12. An example of partly channel destabilized as can be observed in the Western province (see location on Fig. 1).

way. The described events initiated at the shelf break, near the head of the Rosetta canyon and participated for a very important part to the Rosetta fan edification, interfering with turbiditic processes. The relative chronostratigraphy carried out in this area enhances the importance of mass-wasting processes during the building of the Rosetta fan. It is clear that these giant slope instabilities occurred in the area of the NDSF where sedimentation rates are the most important, in the close vicinity of the Rosetta canyon. Sediment overloading probably accounts in this area for the most active triggering parameter of slope instabilities, but other factors such as slope over-steepening because of erosion especially within canyons and tributaries, differential sedimentary inputs associated with sea-level variations and climate changes (Ducassou, 2006), or seismic activity could have been important additional factors for generating slope failures. The clear vicinity of gas chimneys (as for the central slide complex) nearby the scar of the slides (see Fig. 9) suggests the possibility of pore pressure increases by gas. These pore-pressures could also be modified during sea-level variations. Concerning the seismic activity of the area,

different archaeological studies (El-Araby and Sultan, 2000; Goddio, 2000; Badawy, 2001) evidenced the activity of the Cairo–Alexandria trend. The Dashour seism, SW Cairo, recorded in 1992 and having a Magnitude of 5.9, has for example destroyed Pharos lighthouse and submerged Aboukir lighthouse. The described instabilities having been recorded in the extension of this seismic trend, the fact that possible site effects could have been developed on under-compacted sediments would not be set aside. On the basis of this study, it is not possible to discriminate these possible triggering factors.

Detailed slope stability analysis and geohazard studies on the Egyptian margin would require extensive coring and additional data in some key areas (especially high-resolution seismic data along the central slide complex), but at this state of the study, some tendencies can be depicted

1. Clearly, the slope failures generated by salt-tectonic activity are not very risky, at least in terms of tsunamis, because they are repetitive but limited in size. For seabed installations, however, the problem has to be carefully analysed with additional data.
2. Concerning the small-scale failures associated with levee breaching and ESM, the problem is more or less the same.
3. When considering the central province that is the place of important regional sediment failures probably related to the presence of gas, things are different. In this case, the size of recorded debris flows and overlying creeping layer is very important, and the style of deformations may eventually lead to catastrophic detachment. Also the presence of gas makes the system very instable and favourable to pressurizations. Drilling operations or other installations should thus require serious risk assessment studies.
4. Finally, the Western province has been recently the locus of giant slope instabilities during the Pleistocene and Holocene times whose relicts are still observable on slope gradient maps. In particular the residual scars are still extremely steep and expressed on bathymetry, and slides seem to have followed one another through time. This predicts further retrogressive evolution and even if the sedimentation rates strongly decreased since the construction of Aswan dam, these risks should not be undertaken. Many factors could indeed reactivate these scars or generate new slides, as important pore pressures related to gas ascents, an important seismic event, or the loss of foot-buttresses as already evidenced in some parts of the study area (see for example the pathway of the most expressed channel extending downslope the Rosetta canyon: in some areas, it is emplaced just at the foot of ancient scars, slowly eroding the existing foot-buttress). On 3D seismic data, the presence of extensional faults upslope of the last incisions suggest further retrogressive evolution of these slumps (Mannaerts, personal communication). This area has thus to be carefully analysed when considering exploration targets. Finally, considering the tsunami risks on the Egyptian coast, numerical experiments tend to demonstrate that events as massive as Gl-2 would not be able to generate significant tsunamis on the coast, since the large platform is significantly decreasing the power of a potential wave (Huguen, personal communication; Garziglia et al., 2007).

7. Conclusion

The analysis of recent slope instabilities (Late Pleistocene and Holocene) in the NDSF reveals that the Egyptian margin is the locus of numerous slope failures differing in size and type. Recent failures recorded on bathymetry and/or 3.5 kHz and seismic data have been divided into three types (Fig. 6) that should be refined with additional piston-core studies:

1. Instabilities due to regional gravity gliding and spreading of the Plio-Quaternary cover above mobile Messinian salt layers and related local oversteepenings. These events are small-scale (max. 10 km^2 and 10 m thick) but seem to be extremely frequent.
2. Regional repeated instabilities ($\sim$15,000 km^2 for the central slide complex and $\sim$4500 km^2 for the Rosetta slide complex) probably related to fluid ascents, important sedimentary overloads and/or eustatic variations.
3. Small-scale instabilities resulting from tectonic activity along ESM or from sedimentary failures along channel–levee systems.

References

Abdel Aal, A., El Barkooky, A., Gerrits, M., Meyer, H., Schwander, M., Zaki, H., 2000. Tectonic evolution of the Eastern Mediterranean basin and its significance for hydrocarbon prospectivity in the ultradeepwater of the Nile delta. The Leading Edge, 1086–1102.

Badawy, A., 2001. Status of the crustal stress in Egypt as inferred from earthquake focal mechanisms and borehole breakouts. Tectonophysics 343, 49–61.

Bellaiche, G., Loncke, L., Gaullier, V., Mascle, J., Courp, T., Moreau, A., Radan, S., Sardou, O., 2001. Le cône sous-marin du Nil et son réseau de chenaux profonds: nouveaux résultats (campagne Fanil). C.R. Academie des Sciences Paris 333, 399–404.

Biju-Duval, B., Letouzey, J., Montadert, L., 1978. Variety of margins and deep basins in the Mediterranean. AAPG Bulletin, 293–317.

Bouriak, S., Vanneste, M., Saoutkine, A., 2000. Inferred gas hydrates and clay diapirs near the Storegga Slide on the southern edge of the Voring plateau, offshore Norway. Marine Geology 163, 125–148.

Cita, M.B., Beghi, C., Camerlenghi, A., Kastens, K.A., McCoy, F.W., Nosetto, A., Parisi, E., Scolari, F., Tomadin, L., 1984. Turbidites and megaturbidites from the Herodotus abyssal plain (Eastern Mediterranean) unrelated to seismic events. Marine Geology 55, 79–101.

Cramez, C., Jackson, M.P.A., 2000. Superposed deformation straddling the continental-oceanic transition in deep-water Angola. Marine and Petroleum Geology 17, 1095–1109.

Damuth, J.E., 1980a. Use of high-frequency (3.5–12 kHz) echograms in the study of near-bottom sedimentation processes in the deep-sea: a review. Marine Geology 38, 51–75.

Damuth, J.E., 1980b. Quaternary sedimentation processes in the South China Basin as revealed by echo-character mapping and piston-core studies: The Tectonic and Geologic Evolution of Southeast Asian Seas and Islands. American Geophysical Union. Geophysical Monograph 23, 105–125.

Damuth, J.E., 1994. Neogene gravity tectonics and depositional processes on the deep Niger delta continental margin. Marine and Petroleum Geology 11, 320–346.

Damuth, J.E., Flood, R.D., 1984. Morphology, Sedimentation Processes, and growth pattern of the Amazon Deep-sea fan. Geo-Marine Letters 3, 109–117.

Damuth, J.E., Hayes, D.E., 1977. Echo-character of the East Brazilian continental margin and its relationship to sedimentary processes. Marine Geology 24, 73–95.

Diegel, F.A., Karlo, J.F., Schuster, D.C., Shoup, R.C., Tauvers, P.R., 1995. Cenozoic structural evolution and tectono-startigraphic framework of the northern gulf coast continental margin. In: Jackson, M.P.A., Roberts, D.G., Snelson, S. (Eds.), Salt Tectonics: A Global Perspective, vol. 65. AAPG Memoir, pp. 109–151.

Dolson, J.C., Boucher, P.J., Shann, M.V., 2000. Exploration potential in the offshore Mediterranean, Egypt. Perspectives from the context of Egypt's future resources

and business challenges: EAGE conference on geology and petroleum geology, Malta.

Ducassou, E., 2006. Evolution du sytème turbiditique profond du Nil au cours du quaternaire récent. Thèse de doctorat, université de Bordeaux I, 344 pp.

Ducassou, E., Migeon, S., Mulder, T., Gonthier, E., Murat, A., Bernasconi, S., Duprat, J., Capotondi, L., Mascle, J., 2006. The Nile deep-sea turbidite system: characterization and evolution of sedimentary processes during Late Quaternary, External controls on deep-water depositional systems: climate, sea-level and sediment flux. SEPM-Geological Society of London, London.

Ducassou, E., Murat, A., Capotondi, L., Bernasconi, S., Duprat, J., Mulder, T., Migeon, S., 2007. Multiproxy Late Quaternary stratigraphy of the Nile deep-sea turbidite system—Towards a chronology of deep-sea terrigeneous systems. Sedimentary Geology 200, 1–13.

El-Araby, H., Sultan, M., 2000. Integrated seismic risk map of Egypt. Seismological Research Letters 71, 53–66.

Embley, R.W., 1976. New evidence for occurrence of debris-flow deposits in the deep-sea. Geology 4, 371–374.

Embley, R.W., 1980. The role of mass transport in the distribution and character of deep-ocean sediments with special reference to the North Atlantic. Marine Geology 38, 23–50.

Garziglia, S., Migeon, S., Ducassou, E., Mascle, J., Lebourg, T., Tric, E., 2005. Giant submarine landslides in the Nile deep-sea fan (eastern Mediterranean): an integrated study made from geophysical, sedimentological, geotechnical data, and numerical experiment: 2nd International Symposium "Submarine mass-movements and their consequences", Oslo, September 2005.

Garziglia, S., Ioulalen, M., Migeon, S., Ducassou, E., Mascle, J., Sardou, O., Brosolo, L., 2007. Trigerring factors and tsunamigenic potential of a large submarine mass failure on the western nile margin (Rosetta area, Egypt). In: Lykousis, V., Sakellariou, D., Locat, J. (Eds.), Submarine Mass Movements and their Consequences, Vol. 27, pp. 347–355. Springer Netherlands.

Gaullier, V., Mart, Y., Bellaiche, G., Mascle, J., Vendeville, B., Zitter, T., Prismed II scientific party, 2000. Salt tectonics in and around the Nile deep-sea fan: insights from the PRISMED II cruise. Geological Society, London, Special Publications, vol. 174, pp. 111-129.

Goddio, F., 2000. Archaeology, sediments, earthquakes, and exploration in geophysics: The discovery of the sunken cities of the Alexandria no. 48, 20. Egypt coasts: AGU, Fall Meeting 81.

Hirsch, F., Flexer, A., Rosenfield, A., Yellin-Dror, A., 1995. Palinspatic and crustal setting of the eastern Mediterranean. Journal of Geology 18, 149–170.

Huguen, C., 2001. Déformation récente à actuelle et argilo-cinèse associée au sein de la Ride Méditérranéenne (Méditérranée orientale): PhD thesis, speciality: Marine geology, University of Paris 6, 260 p0.

Jacobi, R.D., 1976. Sediment slides on the Northwestern continental margin of Africa. Marine Geology 22, 157–173.

Loncke, L., 2002. Le delta profond du Nil: structure et évolution depuis le Messinien (Miocène terminal), PhD thesis. université Paris 6, 184.

Loncke, L., Gaullier, V., Bellaiche, G., Mascle, J., 2002. Recent depositional pattern of the NDSF from echo-character mapping. Interactions between turbidity currents, mass-wasting processes and tectonics. AAPG Bulletin 86, 1165–1186.

Loncke, L., Gaullier, V., Mascle, J., Vendeville, B., Camera, L., 2006. The Nile deep-sea fan: an example of interacting sedimentation, salt tectonics, and inherited subsalt paleotopographic features. Marine and Petroleum Geology 23, 297–315.

Loncke, L., Mascle, J., Fanil scientific party, 2004. Mud volcanoes, gas chimneys, pockmarks and mounds in the Nile deep sea fan (Eastern Mediterranean): geophysical evidences. Marine and Petroleum Geology 21, 669–689.

Maldonado, A., Stanley, D.J., 1979. Depositional patterns and late quaternary evolution of two Mediterranean submarine fans: a comparison. Marine Geology 31, 215–250.

Mascle, J., Benkhelil, J., Bellaiche, G., Zitter, T., Woodside, J., Loncke, L., 2000. Marine geologic evidence for a Levantine-Sinai plate, a missing piece of the Mediterranean puzzle. Geology 228, 779–782.

McAdoo, B.G., Pratson, L.F., Orange, D.L., 2000. Submarine landslide geomorphology, US continental slope. Marine Geology 169, 103–136.

Morelli, C., 1978. Eastern Mediterranean geophysical results and implications. Tectonophysics 46, 333–346.

Newton, C.S., Shipp, R.C., Mosher, D.C., Wach, G.D., 2004. Importance of Mass Transport Complexes in the Quaternary development of the Nile Fan, Egypt. Offshore Technology Conference, Houston, Texas. 3–6 May 2004, OTC 16742.

Pecher, I.A., Ranero, C.R., von Huene, R., Minshull, T.A., Singh, S.C., 1998. The nature and distribution of bottom simulating reflectors at the Costa Rican convergent margin. Geophysical Journal International 133, 219–229.

Praeg, D., Mascle, J., Geletti, R., Unnithan, V., Wardell, N., 2007. Seismic evidence of a gas hydrate system on the Nile deep-sea fan. American Geophysical Union. Fall Meeting 2007, abstract V13B-1347.

Pratson, L.F., Laine, E.P., 1989. The relative importance of gravity-induced versus current-controlled sedimentation during the Quaternary along the MidEast, U.S. outer continental margin revealed by 3.5 kHz echo-character. Marine Geology 89, 87–126.

Rebesco, M., Della Vedova, B., Cernobori, L., Aloisi, G., 2000. Acoustic facies of Holocene megaturbidites in the Eastern Mediterranean. Sedimentary Geology 135, 65–74.

Reeder, M.S., Rothwell, R.G., Stow, D.A.V., Kahler, G., Kenyon, N.H., 1998. Turbidite flux, architecture and chemostratigraphy of the Herodotus Basin, Levantine Sea, SE Mediterranean. In: Stoker, M.S., Evans, D., Cramp, A. (Eds.), Geological Processes on Continental Margins: Sedimentation, Mass-Wasting and Stability. Special Publications, vol. 129. Geological Society, London, pp. 19–41.

Rempel, A.W., Buffett, B.A., 1998. Mathematical models of gas hydrate accumulation. In: Henriet, J.P., Mienert, J. (Eds.), Gas Hydrates; Relevance to World Margin Stability and Climate Change. Special Publications, vol. 137. Geologival Society, London, pp. 63–74.

Robertson, A.H.F., 1998. Tectonic significance of Eratosthenes seamount: A continental fragment in the process of collision with a subduction zone in the eastern Mediterranean (Ocean Drilling Program Leg 160). Tectonophysics 298, 63–82.

Ross, D.A., Uchupi, E., 1977. The structure and sedimentary history of the southeastern Mediterranean Sea. AAPG Bulletin 61, 872–902.

Rowan, M.G., Jackson, M.P.A., Trudgill, B.D., 1999. Salt-related fault families and fault welds in the northern Gulf of Mexico. AAPG Bulletin 83, 1454–1484.

Ryan, W.B.F., Hsü, K.J. (Eds.), 1973. Initial Reports of the Deep-Sea Drilling Project. US Government Printing Office, Washington, DC, p. 1447.

Sage, L., Letouzey, J., 1990. Convergence of the African and Eurasian plate in the eastern Mediterranean. In: Letouzey, J. (Ed.), Petroleum and Tectonics in Mobile Belts. Editions Technip, Paris, pp. 49–68.

Salem, R., 1976. Evolution of Eocene-Miocene sedimentation patterns in parts of Northern Egypt. AAPG Bulletin 60, 34–64.

Sloan, E.D., 1990. Clathrate Hydrates of Natural Gases. Marcel Dekker, New York, pp. 286-386.

Stover, S.C., Ge, S., Weimer, P., McBride, B.C., 2001. The effects of salt evolution, structural development, and fault propagation on Late Mesozoic-Cenozoic oil migration: A two-dimensional fluid-flow study along a megaregional profile in the northern Gulf of Mexico Basin. AAPG Bulletin 85, 1945–1966.

Tripsanas, E.K., Bryant, W., Phaneuf, B.A., 2004. Slope-instability processes caused by salt movements in a complex deep-water environment, Bryant Canyon area, northwest Gulf of Mexico. AAPG Bulletin 88, 801–824.

Trudgill, B.D., Rowan, M.G., Fiduk, J.C., Weimer, P., Gale, P.E., Korn, B.E., Phair, R.L., Gafford, W.T., Roberts, G.R., Dobbs, S.W., 1999. The Perdido fold belt, northwestern Gulf of Mexico, part 1: Structural geometry, evolution and regional implications. AAPG Bulletin 83, 88–113.

Vendeville, B.C., 1999. Large-scale gravity gliding and spreading above salt or shale. In: Hanson, K.L., Kelson, K.I., Angell, M.A., Lettis, W.R. (Eds.), Identifying Faults and Determining their Origins, Appendix A. U.S. Nuclear Regulatory Commission (NRC), pp. A207–A232. NUREG/CR-5503.

Vendeville, B.C., Jackson, M.P.A., 1992a. The rise of diapirs during thin-skinned extension. Marine and Petroleum Geology 9, 331–354.

Vendeville, B.C., Jackson, M.P.A., 1992b. The fall of diapirs during thin-skinned extension. Marine and Petroleum Geology 9, 354–371.

Von Huene, R., Pecher, I.A., 1999. Vertical tectonics and the origins of BSRs along the Peru margin. Earth and Planetary Science Letters 166, 47–55.

Worall, D.M., Snelson, S., Bally, A.W., 1989. Evolution of the northern gulf of Mexico, with emphasis on Cenozoic growth faulting and the role of salt. In: Palmer, A.R. (Ed.), The Geology of North America—An Overview, vol. A. Geological Society of America, pp. 97–138.